Penerbit UTHM

© Universiti Tun Hussein Onn Malaysia Publisher's Office

JSMPM

http://publisher.uthm.edu.my/ojs/index.php/jsmpm

e-ISSN : 2821-2843

Journal of Sustainable Materials Processing and Management

Significantly Enhanced Structural, Dielectric and Impedance Properties of BCZT-BFO Sensors

Muhammad Salman Habib[1*], Muhammad Asif Rafiq[1], Adnan Maqbool[1]

[1]Department of Metallurgical and Materials Engineering,
University of Engineering and Technology, G.T Road, Lahore, 5489., PAKISTAN

*Corresponding Author

DOI: https://doi.org/10.30880/jsmpm.2022.02.01.005
Received 10 March 2022; Accepted 13 March 2022; Available online 26 April 2022

Abstract: Multiferroics like [(Ba0.85Ca0.15) (Zr0.1Ti0.9) O3, BCZT] and (BiFeO3, BFO) with stochiometric amount were prepared mixed oxide solid state route adding CuO. The compositions were confirmed by X-ray diffraction technique, FTIR confirmed the formation of bonds and the clear idea of bonding pairs, FESEM supported the results of microstructure, and it was revealed that the addition of CuO increased the densification while it was also served as a sintering agent. The impedance spectroscopy (IS) was the tool that explain the relaxation phenomenon of the composition making agreements with the conduction mechanism that the material can be used as negative temperature coefficient of resistance (NTCR) for the applications of capacitors, sensors, actuators, and energy devices.

Keywords: Impedance spectroscopy, sensors, actuators, ferroelectric, perovskite, piezoelectric

1. Introduction

Materials that retain their properties by increasing the environmental factors are termed as sustainable materials. These are high productive, cost efficient, sustain to store energy without changing its structure at a particular temperature. Piezoelectric ceramics are widely used for sensors, actuators, and transducers devices. Piezoelectric are the materials that convert electrical stimulus to mechanical energy [1]. Sensors, actuators, transducers are the energy devices that are utilized in electronic equipment, we can study the response of the materials towards different properties. A sensor can generate current when force is applied on it or vice versa [2]. Lead containing ceramics are serving good applications towards these as they contain the required properties, and it covers mostly 65 % of the piezoelectric materials [3]. Due to the production of lead and the byproducts obtained are carcinogenic, lead free ceramics are investigated and researchers have found that there are number of such variants that will give a possible good agreements for the lead based ceramics [4]. Recently, the studies for the lead-free ceramic based sensors are underway by number of scientist as lead is one of the carcinogenic material that will create environmental issues and human health [5-8]. Research have find out some of the alternatives that are $Bi_{0.5}Na_{0.5}TiO_3$ [9], $BiFeO_3$-$BaTiO_3$ [10], $0.5Ba_{0.8}Ca_{0.2}TiO_3$-$0.5BaTi_{0.8}Sn_{0.2}O_3$-$0.02Pr_6O_{11}$ [11], and $(Na_{0.5}Bi_{0.5})TiO_3$-$SrTiO_3$ [12]. Bismuth Ferrite ($BiFeO_3$) having an extraordinary polarization 100 $\mu C/cm^2$ among its group of leadfree-piezoelectric materials, having a rhombohedral perovskite structure with a high curie temperature of 800 ℃ [13]. The emerging problem with $BiFeO_3$ is the formation of Fe^{+2} and Fe^{+3} and the formation of Bi^{3+} explains the volatilization. This is the way its applications are limited. The application of bismuth ferrite is thus limited to low temperature and low voltages [14].

Principally, dielectric, ferro-electric (FE), anti-ferroelectric (AFE), and relaxor ferroelectric (RF) are some of the categorizations of dielectric materials that can store energy and used for energy harvesting applications at high temperature for long times [15-17]. For the manufacturing and incorporation of electronic devices, several formations have been reported in literature of ABO_3 type solid solutions for ceramic based materials are developed [18-20]. One of the classes is to make a solid solution consisting of BCZT-BFO, BZT-BFO, BT-BFO, BNT-BFO. Including BFO in the

*Corresponding author: salmanhabib2000@gmail.com

ceramic will enhance its magnetic properties as findings have been reported [21]. This will play an enhance role for the magnetic, dielectric, and ferroelectric properties of a material and it can be utilized to make capacitors, sensors, energy devices and manipulated in microelectromechanical systems (MEMS).

In the review we specify the lead-free ceramic materials with its never-ending applications that are utilized by number of fields. In the present study 0.98BCZT-0.02BFO (BCZT-BFO) ceramics were prepared by solid state method. Adding some variants of CuO will change the properties significantly. It was reported that induction of CuO enhances the energy storage ability of the sensors, make it achievable at low temperature, and has a great effect on the morphology.

2. Experimental

The conventional solid-state route was utilized to prepare the barium calcium zirconium titanate [$(Ba_{0.85}Ca_{0.15})(Zr_{0.1}Ti_{0.9})O_3$, BCZT] and bismuth ferrite ($BiFeO_3$, BFO). Precursors $BaCO_3$ (Riedel-de Haën® ≥ 99.5 %), $CaCO_3$ (Sigma-Aldrich® ≥ 99 %), ZrO_2 (UniChem® ≥ 99 %), TiO_2 (AlfaAeser® ≥ 99.5 %), Bi_2O_3 (Merck® ≥ 99.8 %), Fe_2O_3 (Riedel-de Haën® 99.5 %), and CuO (Analar® ≥ 99.8 %) were taken stoichiometrically, weighted, milled at 4h in aqueous inert media using methanol, dried at 80 ℃. The powdered obtained was milled to reduce the particle size considering the same parameters and adding CuO amounts varyingly from 8 % and 10 %. The conventional mixing of BCZT-BFO was also done using ball mill having zirconia balls to reduce the particle size, pressed under ~6.5 Psi pressure to form cylinders (thickness, t = 2 mm and diameter, Ø= 10 mm) sintered in range of 1070-1100 ℃ for 5 h in box furnace to achieve the maximum density.

$$0.85BaCO_3 + 0.15CaCO_3 + 0.1ZrO_2 + 0.9TiO_2 \rightarrow (Ba_{0.85}Ca_{0.15})(Zr_{0.1}Ti_{0.9})O_3 + CO_2(\uparrow) \quad (1)$$

$$Bi_2O_3 + Fe_2O_3 \rightarrow BiFeO_3 + CO_2(\uparrow) \quad (2)$$

Crystalline structure of all prepared solid solutions was analyzed via (PANalytical) X–ray diffractometer (XRD) with Ni-filtered Cu-Kα radiation. Nature of bonding, its functional groups and molecular vibrations in solid solutions was studied via Fourier transform infrared spectrometer (FTIR; Agilent CaryTM 4 630). Field emission scanning electron microscopy (FESEM; Nova NanoSEMTM 450) was done at 5.00 kV to examine the morphology of crystalline structure while high temperature A.C. impedance measurements were done in the range of 100 Hz to 1 MHz via impedance analyzer (TonghuiTM LCR–TH–2829C). Prior to electrical measurements silver paste electrodes were made on both surfaces of pellets by firing at 100 °C for 30 min.

3. Results and Discussion

3.1 XRD Analysis

Fig. 1 shows the room temperature XRD patterns of BCZT-BFO with CuO (8-10 %) optimized at angles of 26º-34º. It was observed that solid solutions of BCZT-BFO prepared successfully and the impurities that are emerging in BFO are suppressed by the BCZT. While adding CuO will make an extra shift in the angles to a higher 2-theta angle. With the addition of CuO, the ionic radius of Cu2 + (0.57 Å / CN4, 0.65 Å / CN5, 0.73 Å / CN6) is much larger than the ionic radius of Asite ions (Ba2 + 1.35 Å, Ca2 + 0.99 Å and Bi2 +). Will be smaller. 1.38 Å) and close to Bsit ions (Ti4 +0.68 Å, Zr4 +0.79 and Fe3 +0.645). Cu2 + replaces B-site ions (Ti4 +, Zr4 +, or Fe3 +), increasing the likelihood of forming a stable solid solution.[22-24]. It was also observed that the phases of BFO will be depressed by the addition of impurity[25].

3.2 FTIR Analysis

The molecular fingerprint regions and the functional groups can be identified by the infrared spectrum of radiation as presented in Fig. 2. The functional group region (FGR) from wavenumber (3500-1500 cm^{-1}) and the fingerprint region (FPR) having wavenumber 1500-400 cm^{-1} [26,27]. BCZT peaks observed in the range of 700-500 cm^{-1} verifies the formation of metal oxide bonding (M-O) such as Ba-O, Ca-O, Zr-O and Ti-O. Fe-O stretching peaks were also observed from peaks 700-730 cm^{-1} is good agreement of the formation of Bi-Fe-O structure. Small spectral shift were observed by the addition of CuO in the ceramic and the confirmations of BCZT-BFO solid solutions [7,28,29]. The spectral shifts clearly explains that the melting point of the BCZT-BFO decreased due to the addition of the impurity phase that impregnate in the structure.

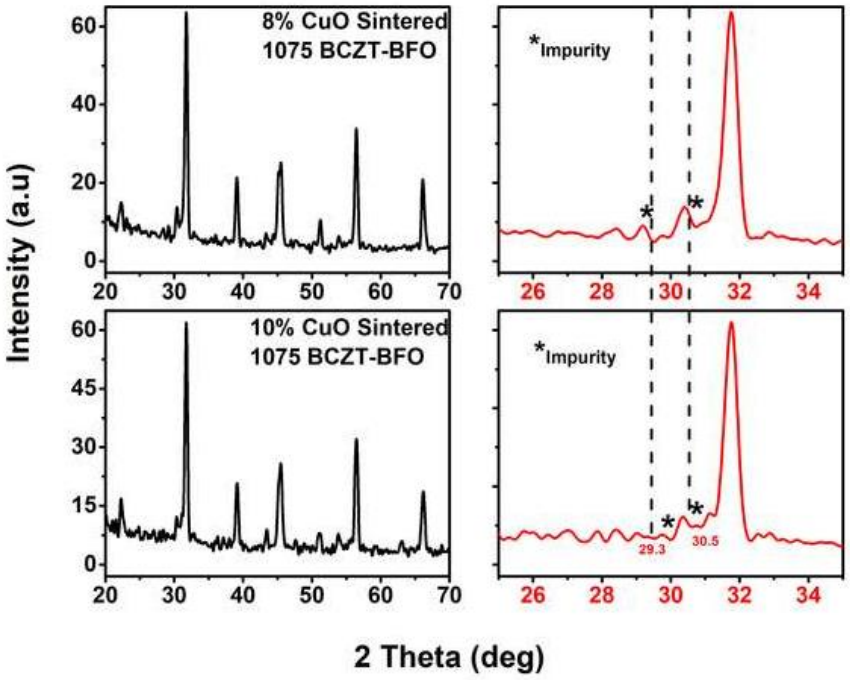

Fig. 1 - XRD patterns of sintered BCZT-BFO at 1075 ℃. The enlarged phase shift angles for the 8-10 % CuO can be seen sideways

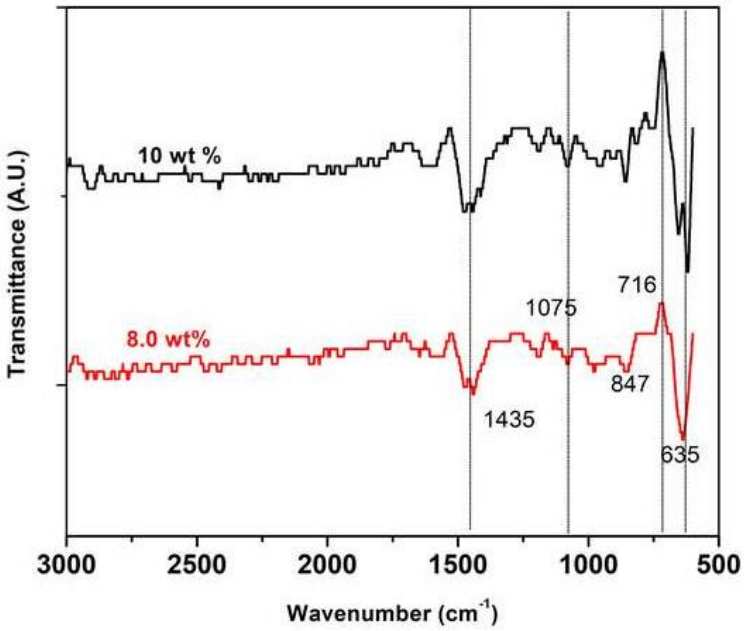

Fig. 2 - FTIR spectrum of BCZT-BFO sintered ceramics

3.3 FESEM Analysis

The prepare pellets were characterized by FESEM and it was found that CuO served as a densification agent for the samples. The addition of more CuO will promote the grains to be more equiaxed and the density of samples were increased as shown from the Fig. 3. In the Fig. 3, the grain size can easily be predicted to equiaxed with addition of CuO in 2(a,b) the grain size is more enlarged and the densification is much higher. The presence of liquid phase will act as a capillary to improve the density of the grains with additionally promoting the sintering to be done at lower agents. It was observed by many of the researchers that the CuO promotes the sintering to lower temperature [30,31]. It was clearly explained that the addition of CuO in the barium titatane based ceramics will act as a sintering aid and will improve the densification. It was further explained that the addition of sintering agent will produce strain on the overall structure of the BCZT-BT family.

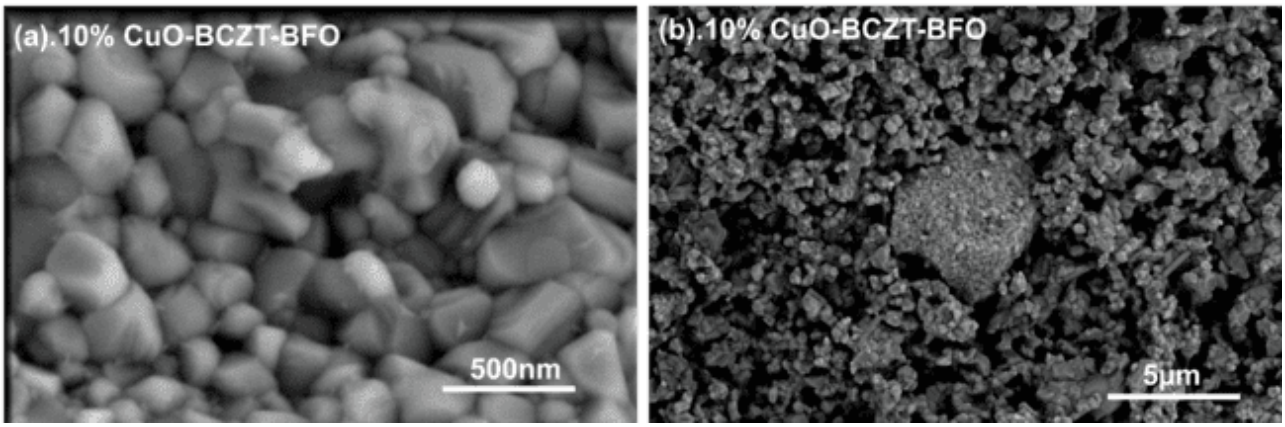

Fig. 3 - Surface morphology of the BCZT-BFO 8%-10% CuO ceramics

3.4 Impedance Spectroscopy

To observe the phenomenon for the contribution of grain and grain boundaries effect impedance spectroscopy is the key tool that will explain the correlated properties of the ceramics. They usually consist randomly oriented grains (g), that are joined together to form grain boundaries (gb). The technique gives the results of electrical impedance which is the combined effect of resistance and reactance. The impedance as a function of frequency explains the behavior or response of the ceramic materials [17,32,33].

Figure shows the real (Z) and imaginary (Z') part of the solid ceramics which behave as insulator at room temperature and dielectric at high temperature. The graphs were plotted from room temperature to 500 ℃ having frequency range from 100 Hz to 1 MHz. Two semicircles were observed, 1st for the grain and the 2nd for the grain boundary. The semicircle at higher frequencies explains the contribution of grains and the semicircles at lower frequencies give idea about the grain boundaries. The conduction mechanism for this is hopping charge mechanism [7,34-36].

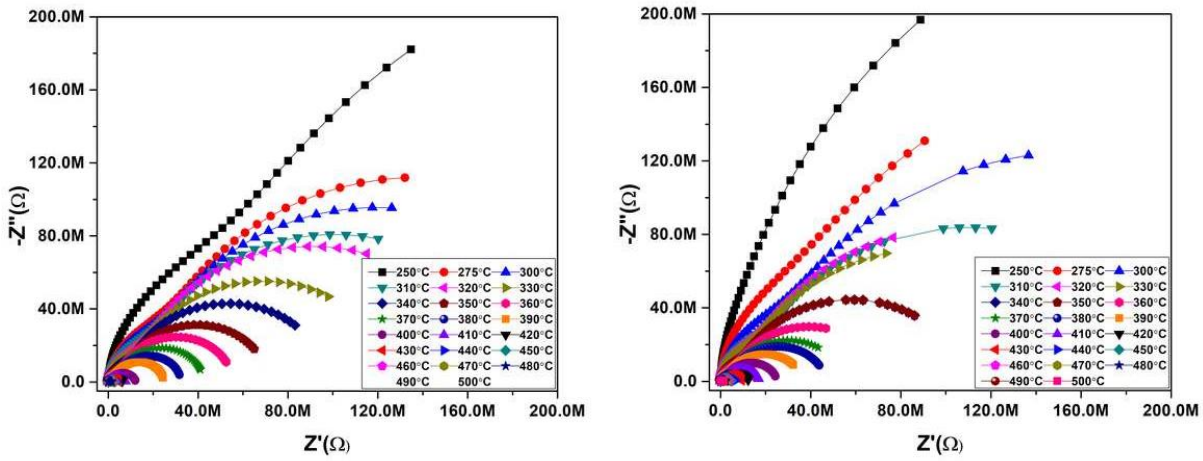

(a) Grain (b) Grain boundary

Fig. 4 - Nyquist plots showing the behavior of ceramics forming two semi-circles

At lower frequencies the region of semicircular arcs decreases as the temperature increases that is a good agreement for the negative temperature coefficient of resistance (NTCR). The relaxation phenomena can be explained by the graphs of frequency with the real and imaginary part of the impedance, and it was observed again, increasing frequencies with increasing temperature for the real part while the curves will shift towards lower values for imaginary part by increasing the frequency and temperatures [2,23,37].

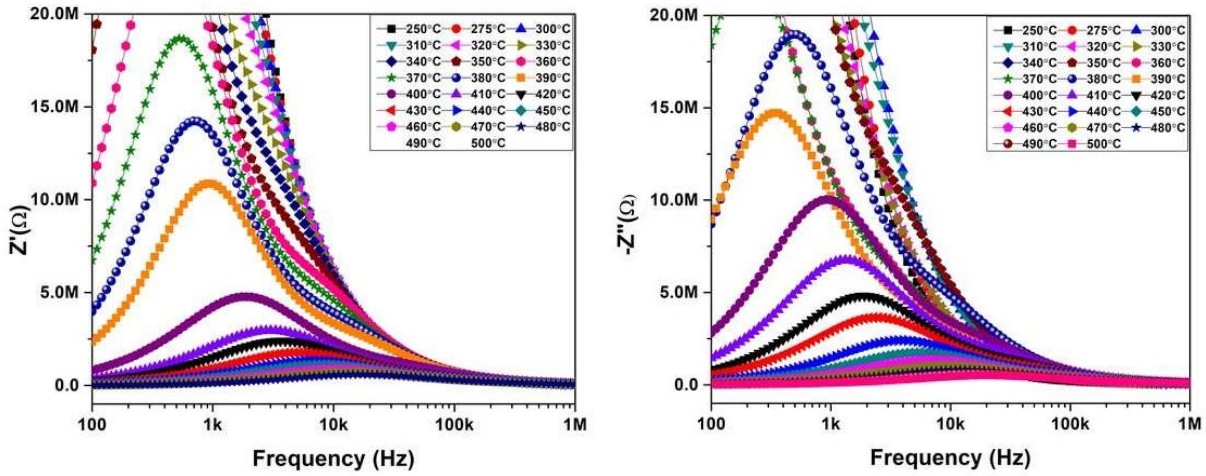

Fig. 5 - Frequency with the real part of the impedance showing that at higher temperatures all the lines merge

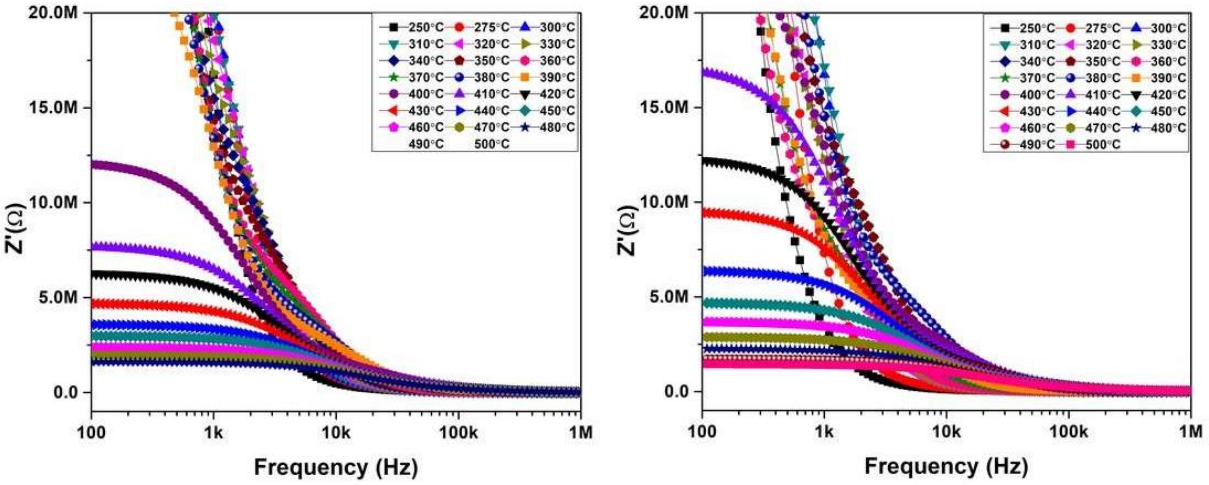

Fig. 6 - Frequency with the real part of the impedance shows that the lines merge at higher temperature having properties of NTCR

4. Conclusion

The pure BCZT-BFO ceramics are prepared via mixed oxide solid state synthesis. XRD and FTIR measurements confirms the pure tetragonal structure of BCZT-BFO ceramics. and the microstructural, dielectric and impedance properties have been studies and it was found that the addition of CuO will enhance the densification by limiting the grain boundaries. The Nyquist plots explain that the grain dominates at the higher frequencies and the grain boundaries at the lower frequencies with temperature vice versa. The conduction mechanism for the BCZT-BFO is hopping conduction that can be explained with the frequency and the real and imaginary part of the impedance. As the temperature increases the impedance decreases with increasing frequencies predicts the negative temperature coefficient of resistance (NTCR). It was demonstrated that the addition of CuO improves the dielectric, microstructural, and impedance properties of the ceramics that are used for the capacitors, dielectrics and other applications.

Acknowledgement

The author could like to acknowledge the Department of Metallurgical and Materials Engineering, University of Engineering and Technology, G.T Road, Lahore.

References

[1] Zhu, L. F., Zhang, B. P., Li, S., Zhao, L., Wang, N., & Shi, X. C. (2016). Enhanced piezoelectric properties of Bi (Mg1/2Ti1/2) O3 modified BiFeO3–BaTiO3 ceramics near the morphotropic phase boundary. *Journal of Alloys and Compounds*, *664*, 602-608.

[2] Tuan, D. A., Tung, V. T., Chuong, T. V., & Hong, L. V. (2015). Properties of lead-free BZT–BCT ceramics synthesized using nanostructured ZnO as a sintering aid. *International Journal of Modern Physics B*, *29*(32), 1550231.

[3] Puli, V. S., Pradhan, D. K., Riggs, B. C., Adireddy, S., Katiyar, R. S., & Chrisey, D. B. (2014). Synthesis and characterization of lead-free ternary component BST–BCT–BZT ceramic capacitors. *Journal of Advanced Dielectrics*, *4*(02), 1450014.

[4] Kaynak, C. B., Lukosius, M., Tillack, B., Wenger, C., Blomberg, T., & Ruhl, G. (2011). Single SrTiO3 and Al2O3/SrTiO3/Al2O3 based MIM capacitors: Impact of the bottom electrode material. *Microelectronic Engineering*, *88*(7), 1521-1524.

[5] Rafiq, M. A., Waqar, M., Muhammad, Q. K., Waleed, M., Saleem, M., & Anwar, M. S. (2018). Conduction mechanism and magnetic behavior of Cu doped barium hexaferrite ceramics. *Journal of Materials Science: Materials in Electronics*, *29*(6), 5134-5142.

[6] Hanani, Z., Ablouh, E. H., Mezzane, D., Fourcade, S., & Gouné, M. (2018). Very-low temperature synthesis of pure and crystalline lead-free Ba. 85Ca. 15Zr. 1Ti. 9O3 ceramic. *Ceramics International*, *44*(9), 10997-11000.

[7] Parida, K., Dehury, S. K., & Choudhary, R. N. P. (2017). Electrical, optical and magneto-electric characteristics of BiBaFeCeO6 electronic system. *Materials Science and Engineering: B*, *225*, 173-181.

[8] Chen, Z. H., Li, Z. W., Ding, J. N., Qiu, J. H., & Yang, Y. (2017). Piezoelectric and ferroelectric properties of Ba0. 9Ca0. 1Ti0. 9Sn0. 1O3 lead-free ceramics with La2O3 addition. *Journal of Alloys and Compounds*, *704*, 193-196.

[9] Yan, F., Bai, H., Shi, Y., Ge, G., Zhou, X., Lin, J., ... & Zhai, J. (2021). Sandwich structured lead-free ceramics based on Bi0. 5Na0. 5TiO3 for high energy storage. *Chemical Engineering Journal*, *425*, 130669.

[10] Habib, M., Iqbal, M. J., Lee, M. H., Akram, F., Gul, M., Zeb, A., ... & Song, T. K. (2022). Piezoelectric performance of Zr-modified lead-free BiFeO3-BaTiO3 ceramics. *Materials Research Bulletin*, *146*, 111571.

[11] Li, Z. W., Ma, M. G., Li, C. B., Chen, Z. H., & Xu, J. J. (2022). Effect of La2O3 doping on the electrical properties of 0.5 Ba0. 8Ca0. 2TiO3-0.5 BaTi0. 8Sn0. 2O3-0.02 Pr6O11 lead-free ceramics. *Journal of Physics and Chemistry of Solids*, *160*, 110366.

[12] Su, Q., Zhu, J., Ma, Z., Meng, X., Zhao, Y., Li, Y., & Hao, X. (2022). Enhanced energy-storage properties and charge-discharge performances in Sm3+ modified (Na0. 5Bi0. 5) TiO3-SrTiO3 lead-free relaxor ferroelectric ceramics. *Materials Research Bulletin*, *148*, 111675.

[13] Sivaraj, K. S., Sreehari, K. S., Bhowmik, R. N., & Anantharaman, M. R. (2021). Sillenite phase stabilized ferromagnetic ordering in multiphasic magnetoelectric bismuth ferrite. *Journal of Solid State Chemistry*, *299*, 122162.

[14] Camargo, J., Espinosa, A. P., Zabotto, F., Ramajo, L., & Castro, M. (2020). Magnetoelectric interactions in bismuth sodium-potassium titanate-nickel cobalt ferrite lead-free composite ceramics. *Journal of Alloys and Compounds*, *826*, 154129.

[15] Maraj, M., Wei, W., Peng, B., & Sun, W. (2019). Dielectric and energy storage properties of Ba (1− x) CaxZryTi (1− y) O3 (BCZT): a review. *Materials*, *12*(21), 3641.

[16] Zaman, A., Hussain, A., Malik, R. A., Maqbool, A., Nahm, S., & Kim, M. H. (2016). Dielectric and electromechanical properties of LiNbO3-modified (BiNa) TiO3–(BaCa) TiO3 lead-free piezoceramics. *Journal of Physics D: Applied Physics*, *49*(17), 175301.

[17] Hao, S., Yi, J., Chao, X., Wei, L., & Yang, Z. (2016). Multiferroic properties in Mn-modified 0.7 BiFeO3-0.3 (Ba0. 85Ca0. 15)(Zr0. 1Ti0. 9) O3 ceramics. *Materials Research Bulletin*, *84*, 25-31.

[18] Sözeri, H., Deligöz, H., Kavas, H., & Baykal, A. (2014). Magnetic, dielectric and microwave properties of M–Ti substituted barium hexaferrites (M= Mn2+, Co2+, Cu2+, Ni2+, Zn2+). *Ceramics International*, *40*(6), 8645-8657.

[19] Meng, B., Miao, Z. Y., Kong, M., Liu, X. X., Yu, J., & Yang, Q. Q. (2014). Microstructure and ionic conductivity of SrTiO3 heterogeneously doped YSZ composite ceramics. *Solid State Ionics*, *258*, 61-66.

[20] Yang, H., Zhou, C., Liu, X., Zhou, Q., Chen, G., Li, W., & Wang, H. (2013). Piezoelectric properties and temperature stabilities of Mn-and Cu-modified BiFeO3–BaTiO3 high temperature ceramics. *Journal of the European Ceramic Society*, *33*(6), 1177-1183.

[21] Park, J. S., Kim, D. J., Chung, W. H., Lim, Y., Kim, H. S., & Kim, Y. B. (2017). Rapid, cool sintering of wet processed yttria-stabilized zirconia ceramic electrolyte thin films. *Scientific Reports*, *7*(1), 1-10.

[22] Xu, Q., Lanagan, M. T., Luo, W., Zhang, L., Xie, J., Hao, H., ... & Liu, H. (2016). Electrical properties and relaxation behavior of Bi0. 5Na0. 5TiO3-BaTiO3 ceramics modified with NaNbO3. *Journal of the European Ceramic Society*, *36*(10), 2469-2477.

[23] Yi, J., Tian, Y., Wei, L., Li, J., Liang, P., Shi, P., ... & Yang, Z. (2015). Structure, dielectric, ferroelectric, and magnetic properties of (1− x) BiFeO3–x (Ba0. 85Ca0. 15)(Zr0. 10Ti0. 90) O3 ceramics. *Materials Research Bulletin*, *66*, 132-139.

[24] Xia, J., Zhao, Q., Chang, A., & Zhang, B. (2015). Synthesis and properties of Mn1. 05− yCo1. 95− x− z− wNixMgyAlzFewO4 NTC ceramic by co-precipitation method. *Journal of Alloys and Compounds*, *646*, 249-256.

[25] Habib, M. S., Rafiq, M. A., Ali, A., Muhammad, Q. K., Shuaib, A., Shahzad, A., ... & Ali, M. M. (2022). Improved sintering and impedance studies of CuO-doped multiferroic (0.98 Ba0. 85Ca0. 15)(Zr0. 1Ti0. 9)· O30. 02BiFeO3 ceramics. *Applied Physics A*, *128*(3), 1-11.

[26] Ji, X., Wang, C., Harumoto, T., Zhang, S., Tu, R., Shen, Q., & Shi, J. (2020). Structure and electrical properties of BCZT ceramics derived from microwave-assisted sol–gel-hydrothermal synthesized powders. *Scientific Reports*, *10*(1), 1-8.

[27] Verma, R., Chauhan, A., Batoo, K. M., Kumar, R., Hadi, M., & Raslan, E. H. (2021). Structural, morphological, and optical properties of strontium doped lead-free BCZT ceramics. *Ceramics International*, *47*(11), 15442-15457.

[28] Acosta, M., Novak, N., Rojas, V., Patel, S., Vaish, R., Koruza, J., ... & Rödel, J. J. A. P. (2017). BaTiO3-based piezoelectrics: Fundamentals, current status, and perspectives. *Applied Physics Reviews*, *4*(4), 041305.

[29] Rafiq, M. A., Rafiq, M. N., Ahmed, F., Ali, L., & Anwar, M. Y. (2014). Structure, Dielectric and Impedance Studies of Li Doped (K0. 5Na0. 5) NbO3 Ceramics. *Journal of Faculty of Engineering & Technology*, *21*(1), 167-178.

[30] Tang, X., Tian, H., Wang, J., Wong, K. H., & Chan, H. L. W. (2006). Effect of $CaRuO_3$ interlayer on the dielectric properties of Ba (Zr, Ti) O_3 thin films prepared by pulsed laser deposition. *Applied Physics Letters*, 89, 1-3.

[31] Chen, T., Zhang, T., Wang, G., Zhou, J., Zhang, J., & Liu, Y. (2012). Effect of CuO on the microstructure and electrical properties of Ba0. 85Ca0. 15Ti0. 90Zr0. 10O3 piezoceramics. *Journal of Materials Science*, *47*(11), 4612-4619.

[32] Muhammad, Q. K., Waqar, M., Rafiq, M. A., Rafiq, M. N., Usman, M., & Anwar, M. S. (2016). Structural, dielectric, and impedance study of ZnO-doped barium zirconium titanate (BZT) ceramics. *Journal of Materials Science*, *51*(22), 10048-10058.

[33] Coondoo, I., Panwar, N., Vidyasagar, R., & Kholkin, A. L. (2016). Defect chemistry and relaxation processes: effect of an amphoteric substituent in lead-free BCZT ceramics. *Physical Chemistry Chemical Physics*, *18*(45), 31184-31201.

[34] Naveed, M., Mumtaz, M., Khan, R., Khan, A. A., & Khan, M. N. (2017). Conduction mechanism and impedance spectroscopy of (MnFe2O4) x/CuTl-1223 nanoparticles-superconductor composites. *Journal of Alloys and Compounds*, *712*, 696-703.

[35] Kumar, K., & Loganathan, A. (2017). The structural, electrical and magnetic properties of Co2+ content dependent Mg-Sr nanoferrite for electromagnetic induction. *Materials Science and Engineering: B*, *224*, 48-55.

[36] Khare, A., Yadava, S. S., Gautam, P., Kumar, A., Mukhopadhyay, N. K., & Mandal, K. D. (2018). Dielectric properties of nanocomposite based on bismuth copper titanate. *Journal of the Australian Ceramic Society*, *54*(1), 139-147.

[37] Wang, X., Liang, P., Chao, X., & Yang, Z. (2015). Dielectric properties and impedance spectroscopy of MnCO3-modified (Ba0. 85Ca0. 15)(Zr0. 1Ti0. 9) O3 lead-free ceramics. *Journal of the American Ceramic Society*, *98*(5), 1506-1514.